Synthesis and Structural Profile Analysis of the MgO Nanoparticles Produced Through the Sol-Gel Method Followed by Annealing Process

by

ORIENTAL JOURNAL OF CHEMISTRY
An International Open Free Access, Peer Reviewed Research Journal
www.orientjchem.org
Est. 1984
ISSN: 0970-020 X
CODEN: OJCHEG
2018, Vol. 34, No.(2):
Pg. 1016-1025

Synthesis and Structural Profile Analysis of the MgO Nanoparticles Produced Through the Sol-Gel Method Followed by Annealing Process

I WAYAN SUTAPA[1]*, ABDUL WAHID WAHAB[2], PAULINA TABA[2] and NURSIAH LA NAFIE[2]

[1]Department of Chemistry, Faculty Mathematic and Natural Science, University of Pattimura Jl. Ir. Putuhena Poka Ambon-Maluku- Indonesia.
[2]Department of Chemistry, Faculty Mathematic and Natural Science, University of Hasanuddin Jl. Perintis Kemerdekaan 90245, Makassar-Indonesia.
*Corresponding author E-mail: wayansutapa@fmipa.unpatti.ac.id

http://dx.doi.org/10.13005/ojc/340252

(Received: October 04, 2017; Accepted: January 20, 2018)

ABSTRACT

MgO nanoparticle was synthesized by sol-gel method from magnesium acetate and oxalic acid dissolved in methanol followed by annealed process. Characterization of functional groups was perform using (FTIR) Fourier Transforms Infrared spectroscopy, crystal profile analysis using (XRD) X-ray Diffraction and morphology using (SEM) Scanning Electron Microscopy. The FTIR and XRD results indicated that the magnesium acetate converted into magnesium oxalate (Precursor), and then the anneal process was changed into MgO nanoparticles. The Scherrer's equation used to determine the distribution of MgO nanoparticle crystals. Modified Williamson-Hall plot is used to determine the strain, stress and energy density value (micro structural properties) based on angle values 2θ and (FWHM) Full width at half maximum of XRD angles from 10° to 80°. The results of the XRD and SEM analysis show that magnesium complexes have changed. The solid layer formed by the Mg polymer complex network is transformed into a cubic structure.

Keywords: MgO nanoparticles, Sol-gel method, Crystallite sizes, Lattice strain, Energy density.

INTRODUCTION

Metal oxides have become the attention of several researchers in last few years due to its potential in many field applications[1–5]. In recent year, researches have focused on synthesis of MgO nanoparticle due to have unique properties there are has a high ionic nature the crystal structure and stoichiometry is simple, large specific surface area, highly reactive due to the large number of active sites, the size and shape of the particles can be varied as needed, and the surface has many

crystal defects. Properties of these materials can be analyzed by computational or conventional method[6–9].

Magnesium oxide was used in many applications such as antibacterial against foodborne pathogen, catalyst and catalyst supports, ceramics, toxic waste remediation, paint, superconductor product and adsorbent[1,3,10]. Generally, various kinds of fabrication method are employed to synthesize MgO nanoparticles such as solution combustion method[11], micro emulsion method[12] deposition of chemical vapour method[13], ablation using laser light method[14], pulsed laser deposition (PLD) method[15], microwave method[16], hydrothermal method[17], co-precipitation method[18], solvothermal reduction[19], thermal decomposition[20], and sol gel method[21,22].

Among these methods, the sol-gel method is one of the most preferred method for synthesizing MgO nanoparticles due to several reason: simple process, high product yield, and low reaction temperature required[23]. In addition the sol gel is inexpensive method to get nano-size MgO with narrow size distribution and larger surface area is very important to solve the problem low reactivity and catalytic ability. The sol gel synthesis of MgO nanoparticle is generally followed by annealed process at the certain temperature. Increased defects of metal oxide crystals can occur in the annealing process because at high temperatures restructuring of the oxide will occurred. The formation of crystal defects on the solids surface will be able to produce active sites that serve as centers for donating their electrons, affecting the surface basicity of MgO produced and increasing the crystallite size[24]. Changes in the microstructures properties require further characterization and calculation to be understood in depth.

In previous studies, MgO nanoparticles was synthesized by sol gel method using magnesium acetate dissolved in ethanol, oxalate and tartrate acid as complexion agent. The formation MgO nanoparticle by this route can result the average crystallite size less than 100 nm for both complexion agent[25]. Based on our study no report the effect of methanol solution in synthesize of MgO nanoparticle. Likewise, the determination of microstructural properties of MgO nanoparticles until now has not been reported.

In this study we have synthesized MgO nanoparticle using methanol to dissolve of magnesium acetate and oxalate acid as complexion agent then annealed at 550 °C for 6 hours. The study also investigated of average size of the crystal, particle size distribution, strain value calculation, stress value and amount of energy crystal density (microstructure properties) that resulted by nanoparticles products.

MATERIALS AND METHODS

Materials

$Mg(CH_3COO)_2$ Magnesium acetate tetrahydrate (Merck & Co. with purity 99.5%); $C_2O_4.2H_2O$ (oxalic acid dehydrate) (Merck & Co. with purity >98 %); and CH_3OH (methanol) (Merck & Co. with purity 99.9%) is used to synthesize the Mg-oxalate precursor to be converted to MgO nanoparticles. All the chemicals used are of analytical grade only.

MgO nanoparticle synthesis

The synthesis procedure of MgO nanoparticles was carried out using the raw material of $Mg(CH_3COO)_2.4H_2O$ and $C_2O_4.2H_2O$. Both of these materials were dissolved using methanol[25]. About 50 g $Mg(CH_3COO)_2.4H_2O$ dissolved in 150 mL of methanol with stirring and heating constantly using magnetic stirrer. The stirring and heating process is stopped until a clear colored mixture is obtained. The resulting mixture is adjusted to pH 5 by adding 1.0 m oxalic acid solution followed by stirring process until the white gel is obtained. The gel is kept in normal room condition and left for one night to make the gelation process is complete. The gel filtered using the filter paper Whatman-42 to separate the gel and its solution. The obtained solid heated at 200 °C for 24 h to remove water and acetate trapped in the formed solids. Furthermore, the dried product is slowly crushed by using mortar and pestle to produce fine powder then was sieved in ±100 mesh to produce a magnesium oxalate complex that serves as a precursor for producing MgO nanoparticles. The complex was formed then annealed at 550 °C at the pressure 1 atm for 6 hours in the furnace. This process will produce nanoparticle crystals MgO.

Characterization methods

FT-IR (Fourier transform infrared)

The functional group of precursor and nanoparticles MgO product was identified by FT-IR. FTIR spectra test is performed using Shimadzu FTIR-8400S Spectrophotometer in range 250-4000 cm^{-1} using KBr pellet.

XRD (X-ray diffraction)

To identify phases and patterns of the magnesium oxalate complex and MgO nanoparticles samples conducted using (XRD) X-ray diffraction the Shimadzu X-ray Diffractometer 9700 (40 kV, 30 mA) with radiation source is CuKα (λ=1.542 Å) and using the filter is nickel with a measurement range of 2θ angle is 10°-80°.

Morphology analysis

The morphology of nanoparticle samples analyzed from images generated by (SEM) scanning electron microscopy with instrument type is JEOL JSM-7600F.

RESULTS AND DISCUSSION

FTIR analysis

FT-IR (Fourier Transform Infrared) spectroscopy was applied to identify of the function group and feature of Mg-oxalate and MgO nanoparticles. The sample is scanned at the range of wave numbers at 350 cm^{-1} to 4000 cm^{-1}. The FTIR results after dried and annealed samples are presented in Fig. 1. Fig. 1A is shown the peaks at 3408.22 cm^{-1} with strong intensity generated by the O-H group (hydrogen bond) of the existance of hydroxyl groups on the solid surface is due to the presence of an acetate group as a by-product of this reaction. The medium peak at 1670.35, 1643.35 cm^{-1} derived from asymmetric vibrations (v_{as}) of C-O Mg-oxalate complex. The strong peak at 1371.39 cm^{-1} and the very strong peak at 1325.10 cm^{-1} are assigned to symmetry vibration (v_s) C-O and δ(O-C-O). The sharp peak at 831.32 cm^{-1} is derived from vibration (v) of C-C and δ(O-C-O). The medium peak at 420.48 cm^{-1} is corresponding to vibration Mg-O.

Figure 1a is shown the medium peak at 3697.54 cm^{-1}, 3446.79 cm^{-1} are the result of stretching O-H bound to the surface of solids derived from adjacent water molecules. The strong absorption at 443.63 cm^{-1} and the medium peak at 862.18 cm^{-1} are the wave number that characterizes stretching vibrations derived from Mg-O bonds[26,27].

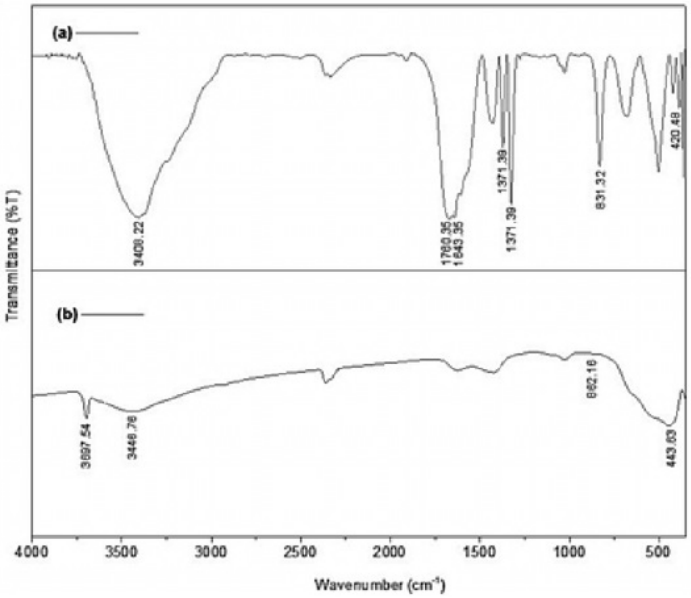

Fig. 1. FTIR spectra of (a) Magnesium oxalate (b) MgO nanoparticles

Decreased of 3408, 22 cm^{-1} strong peak (Fig. 1a) in (Fig. 1b), then peak at 443,63 cm^{-1} (Fig. 1b) is stronger than 420, 48 cm^{-1} (Fig. 1a) due to antisymetric stretching in $Mg(OH)_2$ crystal structure. In addition, this fact also serves as indication that the annealing process at 550 °C with pressure 1 atm has resulted transformation of structure compound from hexagonal ($Mg(OH)_2$ form) to cubic (MgO form).

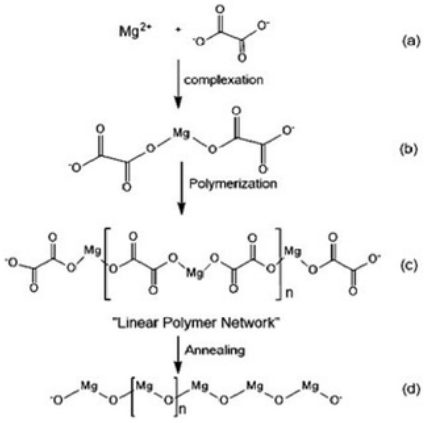

Fig. 2. Growth mechanism for (a-c) Mg-oxalate and (d) MgO nanoparticles[25]

XRD analysis

Powder XRD method was applied to identify the phase and crystallite size of the MgO nanoparticle. The XRD patterns of Mg-Oxalate complex and MgO nanoparticle annealed at 500 °C for 6 h are shown in Fig. 3 and Fig. 4. Fig. 3 shows that the Mg-oxalate complex was formed in this process and these result by XRD. The X-ray result is good agreement to previous result[28]. The presence other peak diffraction the XRD patterns rise from acetate acid and water remained in the complex.

Figure 4 shows the XRD diffraction pattern of MgO nanoparticles resulted. There is a strong and sharp diffraction peak at 2θ angle of 38.30°, 42.78°, 55.51°, 62.13°, 74.47°, 78.40° corresponding to (1 1 1), (2 0 0), (2 2 0), (2 2 0), (3 1 1), and (2 2 2) plane respectively are indicated of MgO nanoparticle, while diffraction peak located at the 2θ value of 16.96°, 37.00°, 58.68° are indicated $Mg(OH)_2$ compound[29]. The resulting MgO diffraction pattern then matched with The International Centre for Diffraction Data [ICDD No: 01-078-0430].

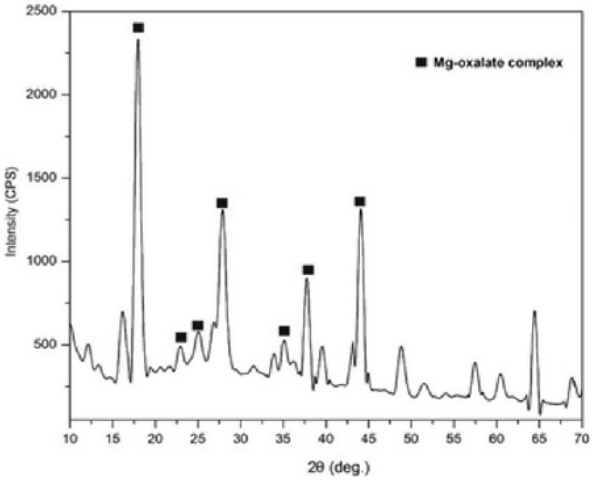

Fig. 3. X-ray diffraction pattern of the Mg-oxalate complex

Subsequently, an average crystal size calculation was performed for each peak resulted on the XRD diffraction. The particle size of nanoparticles determined using Debye – Scherer equation[30].

$$D = \frac{K\lambda}{\beta cos\theta} \quad (1)$$

θ is angle value of each peak, β is the FWHM value, D is the average size of crystal particle, K is Debye-Scherer constant of 0.94, δ is wavelength

value of CuKá radiation of 0.144 nm. The average size of crystal particle calculated for synthesis MgO nanoparticles was 7.51 nm. Based on Debye Scherer equation also can be used determined the dislocation density (δ) of crystal.

The dislocation density (δ) is obtained by determining the length of the dislocation line divided by the crystal volume of the nanoparticles. The value (δ) denotes the number of crystal defects possessed by a solid material. To calculate the dislocation density (δ) can be done using equations[31].

$$\delta = 1/D^2 \qquad (2)$$

The result of the dislocation density (δ) of the synthesized MgO nanoparticles is 0.0097 $(nm)^{-2}$. These results indicate MgO crystal have small dislocation density value. Based on dislocation density value of the MgO nanoparticles obtained in this study, confirmed that the MgO nanoparticle product has a good degree of crystallinity.

Crystallite size distribution

The determination of the size distribution of a crystal is a model resulted from the crystal size effect by assuming the spherical domain sizes is long-normal distribution. Based on observation many researcher the distribution functions has been proven to be effective is defined as[32].

$$f(x) = \frac{1}{\sqrt{2\pi}\,\sigma}\frac{1}{x}\exp\left\{-\frac{[\ln(x/m)]^2}{2\sigma^2}\right\} \qquad (4)$$

x is the value obtained from the distribution of crystal size, σ is the value of variance and med. is the median value obtained from the size distribution function. The volume-area-, is derived from the average value of the crystal size with assuming the crystal form is spherical. These two values are determined using the equation[33]:

$$[x]_{area} = med.\exp(2.5\,\sigma^2) \qquad (5)$$

$$[x]_{volume} = med.\exp(3.5\,\sigma^2) \qquad (6)$$

The crystallite size distribution function of MgO nanoparticles on annealed temperature 550 °C are plotted in Figure 5.

Based on Fig. 5 can be seen that the MgO nanoparticles have distribution particles size lower than 10 nm. Based on calculation result obtained median value and value of variance 1.23 and 6.85

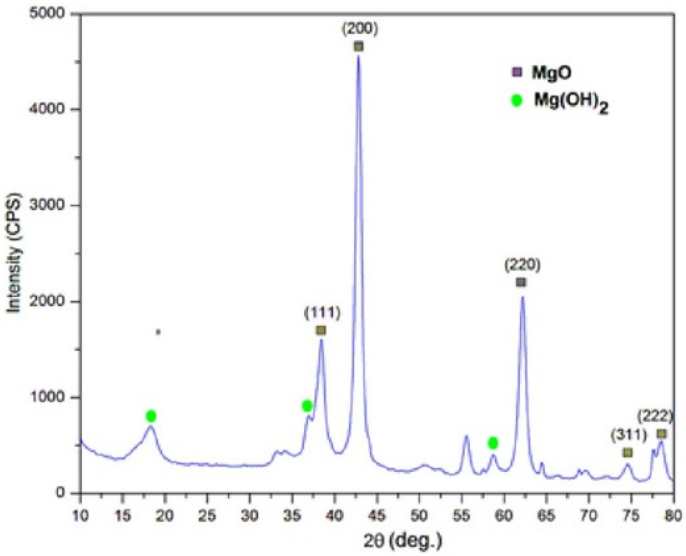

Fig. 4. XRD diffraction patterns of nanoparticles MgO annealed at 550 °C for 6 hours

respectively. This means that the size of crystallite is on a nanometer scale range. While, the size value the area- and the volume- are 293.33 and 1.32 x 10^3 nm, respectively. These value are relatively far each other, its fact also supported by size distribution is wide: $\sigma = 1.2.3$. The volume weight average size is about 1.32 x 10^3 nm, its show that nanocrytalline grain-boundary region or the amorphous part of the specimen contribute mainly to the diffuse background[33].

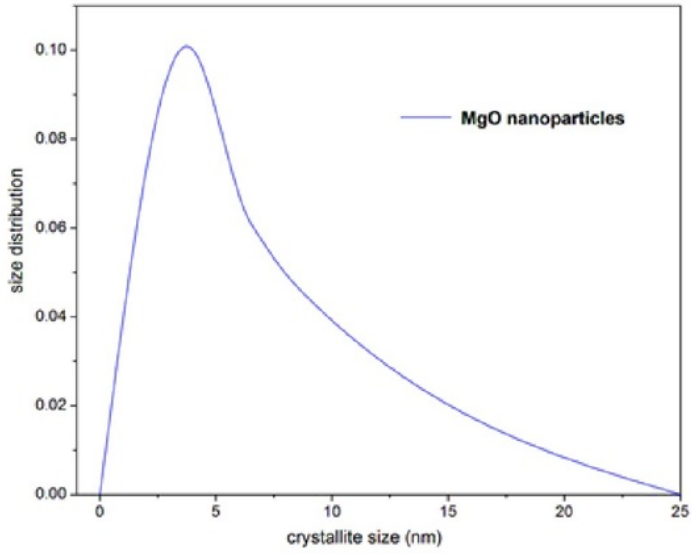

Fig. 5. the crystallite size distribution functions determined by X-rays for MgO nanoparticles powder

Strain, Stress and Energy density of crystal determination of strain (ε)

Calculation of the strain, stress and density of crystal can be solved using (W-H) Williamson–Hall approach. The W-H approach used in this case involves a widened diffraction of peak value, which results from variations in crystal size and strain values. In addition, a widened peak value due to coherent scattering and internal stress values occurs during the sample preparation process. The calculation of the diffraction pattern generated by the widened peak is carried out using the equation 7,[29] β_{hkl} corresponding to each diffraction peak of MgO.

$$\beta_{hkl} = \left[\left(\beta^2_{hkl}\right)_{measured} - \left(\beta^2_{hkl}\right)_{standr}\right]^{1/2} \quad (7)$$

The amount of contribution derived from the size and strain value of material crystal shows the total value of broadening peak. This relationship can be written by the equation:

$$\beta_{hkl}=\beta_D+\beta_C \quad (8)$$

β_D is a value derived from the size of the crystal, β_c is generated by broadening peak due to the occurrence of the induced strain and β_{hkl} is the FWHM value that has been corrected by broadening peak.

$$\beta_{hkl}\cos\theta = \frac{K\lambda}{D} + 4\varepsilon\sin\theta \quad (9)$$

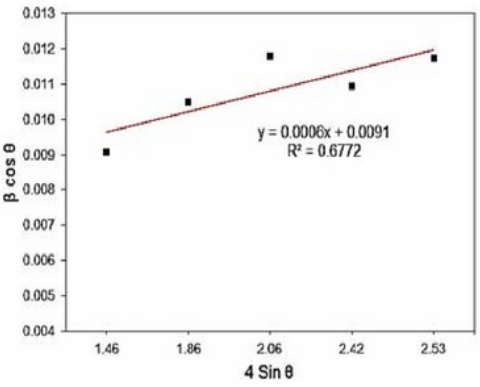

Fig. 6. Plot β_{hkl} cos θ versus 4sinθ

Equation 9 is a form of (UDM) uniform deformation model which uses the assumption that crystals undergo the same strain in all directions of the crystal plane. In addition, this equation also assumes that the character possessed by the crystal is not affected in the direction specified and the crystal is isotropic[29]. The value of micro strain (ε) calculated using the values obtained from the slope of the graph in the linear regression (Fig. 6) is 1.5 x 10^{-4}. The calculation result of micro strain is very low and the straight lines with R^2=0.6772 of the annealed MgO at temperatures of 500 °C were almost horizontal, this suggesting that the nanoparticles product is a lack of strain[34].

Determination Stress of crystal (σ)

Estimation of the stress of crystal is calculated using anisotropic approach, these make Williamson–Hall equation is modied into (USDM) *uniform stress deformation model*. In USDM, using the assumption that the deformations that occur due to stress on all directions of the crystal plane is similar, the micro strain values that occur on particles is very small, and the proportional linearity between stress and strain values is used in Hook's Law σ =εY derived from the stress crystal value, Y is Young modulus value (or) the elasticity of the crystal. Using the Hooke's law and changing the value of strain (ε) in the equation 9, the new equation can be obtained:

$$\beta_{hkl} \cos\theta = \frac{K\lambda}{D} + \frac{4\sigma \sin\theta}{Y} \quad (10)$$

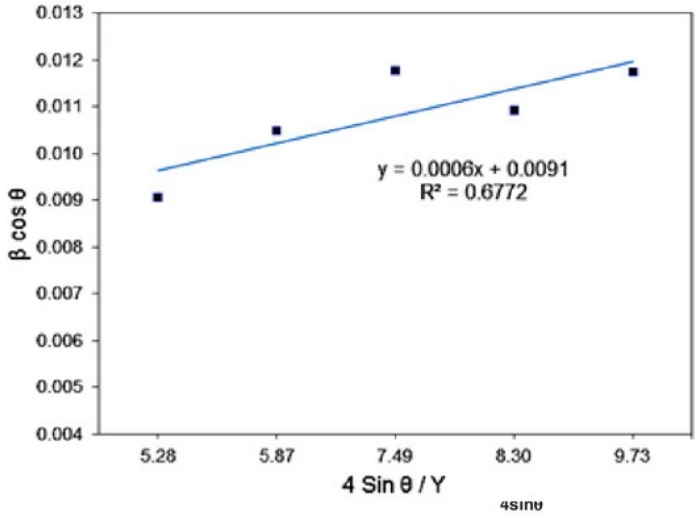

Fig. 7. Plot β_{hkl} cosθ versus $\frac{4\sin\theta}{Y}$

Application the equation can be conducted for materials that have small strain values. Based on the experiment data, Young (Y) Modulus for MgO nanoparticles that has a cubic structure is 248.73 GPa. These data it can be generated graph relation β_{hkl} cos θ versus $\frac{4\sin\theta}{Y}$ as in Fig. 7. The magnitude of stress owned by nanoparticles MgO calculated from the slope of the graph is 37.31 MPa.

Determination of crystal Energy Density (u_{ed})

The crystal Energy Density of a crystal can be determined by (UDEDM) uniform deformation energy density model. Equation (9), assumes that the nature of the homogeneity of the crystals and its isotropic properties. In addition, in this model also considered the energy density value of strain that make the proportionality constant of the relationship between strain-stress is dependent. In an elastic material such that Hooke's law can be applied, the energy density of the material u_{ed} (energy per unit) can be determined by involving the functional value of the strain is $u_{ed}(\varepsilon^2 Y)/2$ Thus, the Equation 11 is resulted from modification of energy relations and strains can be obtained.

$$\beta_{hkl}\cos\theta = \frac{K\lambda}{D} + \left(4\sin\theta\left(\frac{2u_{ed}}{Y}\right)^{1/2}\right) \quad (11)$$

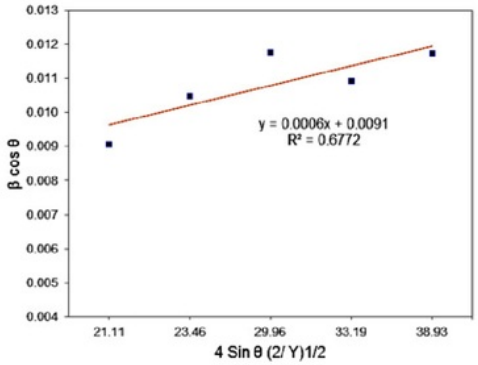

Fig. 8. Plot β_{hkl} cosθ versus 4sin(2/Y)$^{1/2}$

Plots of $\beta_{hkl}\cos\theta$ versus $4\sin\theta\left(\frac{2u_{ed}}{Y}\right)^{1/2}$ is the result of calculation from available data and then the linear regression conducted to obtain a straight line (Fig. 8). Based on the slope value of the graph it can estimate the energy density of the MgO nanoparticles is 0.712 MPa.

Morphological analysis

The SEM image of magnesium oxalate complex and MgO nanoparticle is shown in Fig. 9. SEM analysis was remarkable method for showing the surface morphologies of solid materials. Figure 9a shows that the magnesium oxalate compound complexes produced by sol gel synthesis are solid layers formed by a linear polymer complex network. The process of formation of this linear network complex can be understood by the reaction mechanism of Figure 2 (a-c).

Figure 9b shows the magnesium structure change from magnesium oxalate complex to Mg-O polymer (Fig. 2d). These results show that changes in annealing temperature will affect the morphology and size of the material. After annealing at 550 °C the magnesium morphology changes from the form of the solid layers to the cubic crystal structure. MgO nanoparticles produced through this route by using methanol solvent have a morphological and structural similarity to the process using ethanol solvent[25].

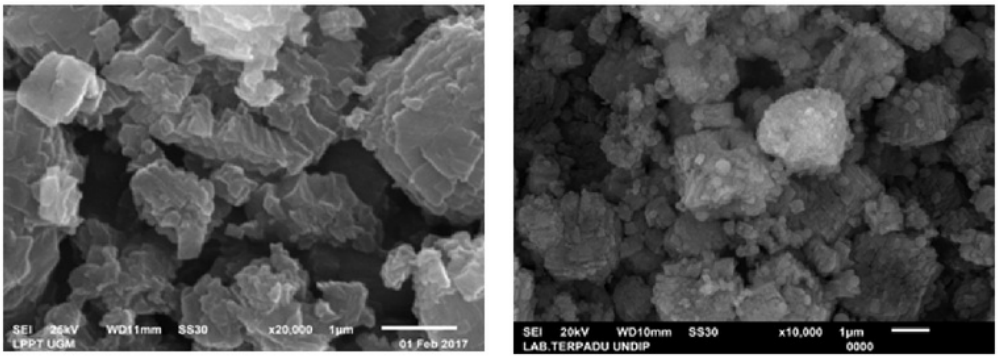

(a) (b)

Fig. 9. SEM of micrograph of (a) Mg-oxalate complex (b) MgO nanoparticles

Estimation of texture coefficient ($TC_{(hkl)}$)

Determination of the texture coefficient is one of methods used to calculate contribution percentage of each peak in XRD diffraction which as a quantitative reference to determine the orientation of each detected crystal. Texture coefficient values also can be used to determine the tendency of the crystal planes in the sample. The coefficient of texture can be calculated using the equation 12

$$TC_{(hkl)} = \frac{I_{(hkl)}/I_{o(hkl)}}{\sum_N I_{(hkl)}/I_{o(hkl)}} \times 100\% \quad (12)$$

$I_{(hkl)}$, $I_{o(hkl)}$ and N are the relative intensity of the sample, the relative intensity of the standard and the XRD diffraction peak number respectively[35,36]. The texture coefficient of MgO nanoparticles annealed at 550 °C for 6 h was calculated. Based on the obtained calculation results can be seen that the coefficient value of the highest MgO nanoparticle texture is 1.13. The highest $TC_{(hkl)}$

value is obtained in the crystal plane (111). The result is indicates that most of the MgO nanoparticles on the sample will be preferred orientation of (111) plane.

CONCLUSION

MgO nanoparticle was synthesized by sol-gel method from magnesium acetate and oxalic acid dissolved in methanol followed by annealed process. Characterization product conducted by FTIR, XRD, and SEM. The synthesis process of sol-gel method has obtained the precursor of Magnesium oxalate. The annealed process at 550 °C for 6 h was annealed magnesium oxalate complex into the MgO nanoparticles. The XRD diffraction peak of MgO nanoparticles analyzed using the Scherrer's equation, the crystallite size distribution, UDM, UDSM, and UDEDM and TC_{hkl}. FTIR result shows that most of the functional group of the magnesium acetate was changed into MgO nanoparticles. The crystallite size distribution the MgO nanoparticles have distribution particles size lower than 10 nm. The size value the area- and the volume- are 293.33 and 1.32 x 10^3 nm. The value of strain(ε), value of stress(σ), and the energy density of MgO nanoparticle crystal (u_{ed}) were calculated from the W–H approach are 1.5 x 10^{-4}, 37.31 MPa, 0.712 MPa respectively. The SEM images showed morphology of Mg oxalate complex and MgO nanoparticles. These images were justifying that most the magnesium oxalate in solid layers formed by a linear polymer complex network change into cubic structure (MgO nanoparticles) with an average particle size of 7.51 nm. TC_{hkl} calculation result is indicates that the MgO nanoparticles on the sample is preferred orientation of (111).

ACKNOWLEDGMENT

Authors are thankful to Ministry of Research, Technology and Higher Education of the Republic of Indonesia, for the Doctoral Grand Program on year 2017 and Scholarship for Postgraduate Education in the Country for nancial assistance to carry out the research.

REFERENCES

1. Duan, G.; Yang, X.; Chen, J.; Huang, G.; Lu, L.; Wang, X. *Powder Technol.,* **2007**, *172*, 27–29.
2. Sutapa, I. W.; Bandjar, A.; Rosmawaty; Sitaniapessy, M. *Int. J. Mater. Sci. Appl.,* **2015**, *4*, 219.
3. Jin, T.; He, Y. *J. Nanoparticle Res.,* **2011**, *13*, 6877–6885.
4. Indulal, C. R.; Biju, R.; Nand, D.; Raveendran, R. *Orient. J. Chem.,* **2017**, *33*, 1545–1549.
5. O.Siyanbola, T.; F.Akinsola, A.; A.Adekoya, J.; O.Ajani, O.; O.Ehi-Eromosele, C.; Olasehinde, G. I. *Orient. J. Chem.,* **2017**, *33*, 09-16.
6. Dercz, G.; Prusik, P.; Paj¹k, L.; Pielaszek, R.; Malinowski, J. J.; Pud³o, W. *Materials Science-Poland,* **2009**, *27*, 201–207.
7. Hadanu, R.; Idris, S.; Sutapa, I. W. *Indones. J. Chem.,* **2015**, *15*, 86–92.
8. Klabunde, K. J.; Stark, J.; Koper, O.; Mohs, C.; Park, D. G.; Decker, S.; Jiang, Y.; Lagadic, I.; Zhang, D. *J. Phys. Chem.,* **1996**, *100*, 12142–12153.
9. Sutapa, I. W.; Armunanto, R.; Wijaya, K. *Indones. J. Chem.,* **2010**, *10*, 184–188.
10. Niu, H.; Yang, Q.; Tang, K.; Xie, Y. *Scr. Mater.,* **2006**, *54*, 1791–1796.
11. Orante-Barrón, V. R.; Oliveira, L. C.; Kelly, J. B.; Milliken, E. D.; Denis, G.; Jacobsohn, L. G.; Puckette, J.; Yukihara, E. G. *J. Lumin.,* **2011**, *131*, 1058–1065.
12. Svensson, E. E.; Nassos, S.; Boutonnet, M.; Järås, S. G. *Catal. Today,* **2006**, *117*, 484–490.
13. Ryu, H.; Singh, B. K.; Bartwal, K. S. Synthesis and Optimization of MWCNTs on Co-Ni/MgO by Thermal CVD. *Adv. Condens. Matter Phys.,* **2008**, 2008, 1-6.
14. Vendamani, V. S.; Tripathi, A.; Pathak, A. P.; Rao, S. V.; Tiwari, A. *Mater. Lett.,* **2017**, *192*, 29–32.
15. Nagashima, K.; Yanagida, T.; Tanaka, H.; Kawai, T. *J. Appl. Phys.,* **2007**, *101*, 124304.
16. Makhluf, S.; Dror, R.; Nitzan, Y.; Abramovich, Y.; Jelinek, R.; Gedanken, A. *Adv. Funct. Mater.,* **2005**, *15*, 1708–1715.
17. Ding, Y.; Zhang, G.; Wu, H.; Hai, B.; Wang, L.; Qian, Y. *Chem. Mater.,* **2001**, *13*, 435–440.

18. Das, S.; Srivasatava, V. C. *Smart Sci.,* **2016**, *4*, 190–195.
19. Ling, Z.; Zheng, M.; Du, Q.; Wang, Y.; Song, J.; Dai, W.; Zhang, L.; Ji, G.; Cao, J. *Solid State Sci.,* **2011**, *13*, 2073–2079.
20. Morozov, S. A.; Malkov, A. A.; Malygin, A. A. *Russ. J. Gen. Chem.,* **2003**, *73*, 37–42.
21. Athar, T. *Mater. Focus,* **2013**, *2*, 493–496.
22. Minami, H.; Kinoshita, K.; Tsuji, T.; Yanagimoto, H. *J. Phys. Chem. C.,* **2012**, *116*, 14568–14574.
23. Mastuli, M. S.; Ansari, N. S.; Nawawi, M. A.; Mahat, A. M. *APCBEE Procedia,* **2012**, *3*, 93–98.
24. Mguni, L. L.; Mukenga, M.; Jalama, K.; Meijboom, R. *Catal. Commun.,* **2013**, *34*, 52–57.
25. Mastuli, M. S.; Kamarulzaman, N.; Nawawi, M. A.; Mahat, A. M.; Rusdi, R.; Kamarudin, N. *Nanoscale Res. Lett.,* **2014**, *9*, 134.
26. Rezaei, M.; Khajenoori, M.; Nematollahi, B. *Powder Technol.,* **2011**, *205*, 112–116.
27. Song, G.; Ma, S.; Tang, G.; Wang, X. *Colloids Surf. Physicochem. Eng. Asp.,* **2010**, *364*, 99–104.
28. Lakshmi Reddy, S.; Ravindra Reddy, T.; Siva Reddy, G.; Endo, T.; Frost, R. L. *Spectrochim. Acta. A. Mol. Biomol. Spectrosc.,* **2014**, *123*, 25–29.
29. Bindu, P.; Thomas, S. *J. Theor. Appl. Phys.,* **2014**, *8*, 123–134.
30. Patterson, A. L. *Phys. Rev.,* **1939**, *56*, 978–982.
31. Khan, Z. R.; Zulfequar, M.; Khan, M. S. *Mater. Sci. Eng. B.,* **2010**, *174*, 145–149.
32. Ungár, T.; Gubicza, J.; Ribárik, G.; Borbély, A. *J. Appl. Crystallogr.,* **2001**, *34*, 298–310.
33. Gubicza, J.; Ribárik, G.; Bakonyi, I.; Ungár, T. *J. Nanosci. Nanotechnol.,* **2001**, *1*, 343–348.
34. Zhang, X.; Zheng, Y.; Feng, X.; Han, X.; Bai, Z.; Zhang, Z. *RSC Adv.,* **2015**, *5*, 86102–86112.
35. Manifacier, J. C.; Gasiot, J.; Fillard, J. P. *J. Phys. [E],* **1976**, *9*, 1002.
36. Wang, J.; Yang, F.; Wei, X.; Zhang, Y.; Wei, L.; Zhang, J.; Tang, Q.; Guo, B.; Xu, L. *Phys. Chem. Chem. Phys.,* **2014**, *16*, 16711–16718.

Synthesis and Structural Profile Analysis of the MgO Nanoparticles Produced Through the Sol-Gel Method Followed by Annealing Process

ORIGINALITY REPORT

%7	%2	%5	%3
SIMILARITY INDEX	INTERNET SOURCES	PUBLICATIONS	STUDENT PAPERS

PRIMARY SOURCES

1	Submitted to The University of Manchester Student Paper	%1
2	S.A Nasser, H.H Afify, S.A El-Hakim, M.K Zayed. "Structural and physical properties of sprayed copper–zinc oxide films", Thin Solid Films, 1998 Publication	<%1
3	Issa M. El-Nahhal, Fawzi S. Kodeh, Jamil K. Salem, Talaat Hammad, Sylvia Kuhn, Rolf Hempelmann, Sara Al Bhaisi. "Silica, Mesoporous Silica and Its Thiol Functionalized Silica Coated MgO and Mg(OH)2 Materials", Chemistry Africa, 2019 Publication	<%1
4	Alexey S. Kurlov, Aleksandr I. Gusev. "Tungsten Carbides", Springer Nature, 2013 Publication	<%1
5	E. Schafler. "Evolution of Microstructure during	<%1

	Thermal Treatment in SPD Titanium", Nanomaterials by Severe Plastic Deformation, 02/25/2004 Publication	
6	Submitted to Yeungnam University Student Paper	<%1
7	Atul K. Prashar, Hwimin Seo, Won Choon Choi, Na Young Kang, Sunyoung Park, Kiwoong Kim, Da Young Min, Hye Mi Kim, Yong Ki Park. " Factors Affecting the Rate of CO Absorption after Partial Desorption in NaNO -Promoted MgO ", Energy & Fuels, 2016 Publication	<%1
8	Mittemeijer, Eric J., and Udo Welzel. "Diffraction Line-Profile Analysis", Modern Diffraction Methods MITTEMEIJER DIFFRACTION O-BK, 2013. Publication	<%1
9	www.ijert.org Internet Source	<%1
10	pt.scribd.com Internet Source	<%1
11	Submitted to SASTRA University Student Paper	<%1
12	S. Lakshmi Reddy, T. Ravindra Reddy, G. Siva Reddy, Tamio Endo, Ray L. Frost. "Synthesis	<%1

and spectroscopic characterization of magnesium oxalate nano-crystals", Spectrochimica Acta Part A: Molecular and Biomolecular Spectroscopy, 2014
Publication

13	Submitted to American University in Cairo Student Paper	<%1
14	Wang, Guozhi, Lei Zhang, Hongxing Dai, Jiguang Deng, Caixin Liu, Hong He, and Chak Tong Au. "P123-Assisted Hydrothermal Synthesis and Characterization of Rectangular Parallelepiped and Hexagonal Prism Single-Crystalline MgO with Three-Dimensional Wormholelike Mesopores", Inorganic Chemistry, 2008. Publication	<%1
15	G. Ribárik. "Dislocation densities and crystallite size distributions in nanocrystalline ball-milled fluorides, MF_2 (M = Ca, Sr, Ba and Cd), determined by X-ray diffraction line-profile analysis", Journal of Applied Crystallography, 11/12/2005 Publication	<%1
16	www.ias.ac.in Internet Source	<%1
17	ijsr.in Internet Source	<%1

18	Submitted to Universiti Teknologi MARA Student Paper	<%1
19	krex.k-state.edu Internet Source	<%1
20	duepublico.uni-duisburg-essen.de:443 Internet Source	<%1
21	Gourav Singla, K. Singh, O. P. Pandey. "Williamson–Hall study on synthesized nanocrystalline tungsten carbide (WC)", Applied Physics A, 2013 Publication	<%1
22	nopr.niscair.res.in Internet Source	<%1
23	Submitted to Institute of Graduate Studies, UiTM Student Paper	<%1
24	Jaison, J, C Ashok raja, S Balakumar, and Y S Chan. "Sol – Gel synthesis and characterization of magnesium peroxide nanoparticles", IOP Conference Series Materials Science and Engineering, 2015. Publication	<%1

EXCLUDE QUOTES	ON	EXCLUDE MATCHES	< 5 WORDS
EXCLUDE	ON		

BIBLIOGRAPHY